Geophysical Research Letters

RESEARCH LETTER
10.1029/2023GL106221

Longrui Zhang and Fu Luo contributed equally to this work and share the first authorship.

Key Points:

- Using a short-time Fourier transform to study the multi-timescale evolution of the canopy urban heat island intensity (CUHII)
- Close relationships existed between CUHII and the background meteorological forcing at intra-annual, intra-daily, and weather scales
- The frequency of cold/heat waves in Beijing showed a significant negative correlation with the weather-scale spectral intensity of the CUHII

Supporting Information:

Supporting Information may be found in the online version of this article.

Correspondence to:

Y. Yang,
yyj1985@nuist.edu.cn

Citation:

Zhang, L., Luo, F., Pan, G., Zhang, W., Ren, G., Zheng, Z., & Yang, Y. (2024). Elucidating the multi-timescale variability of a canopy urban heat island by using the short-time Fourier transform. *Geophysical Research Letters*, *51*, e2023GL106221. https://doi.org/10.1029/2023GL106221

Received 1 JUN 2023
Accepted 15 DEC 2023

Author Contributions:

Conceptualization: Yuanjian Yang
Data curation: Longrui Zhang, Fu Luo, Zuofang Zheng
Formal analysis: Longrui Zhang
Funding acquisition: Yuanjian Yang
Resources: Zuofang Zheng, Yuanjian Yang
Supervision: Yuanjian Yang
Visualization: Longrui Zhang

Elucidating the Multi-Timescale Variability of a Canopy Urban Heat Island by Using the Short-Time Fourier Transform

Longrui Zhang[1], Fu Luo[1], Guitao Pan[2], Wenjie Zhang[3,4], Guoyu Ren[5,6], Zuofang Zheng[7], and Yuanjian Yang[1]

[1]Collaborative Innovation Centre on Forecast and Evaluation of Meteorological Disasters, Key Laboratory for Aerosol-Cloud-Precipitation of China Meteorological Administration, School of Atmospheric Physics, Nanjing University of Information Science & Technology, Nanjing, China, [2]Electric Power Evaluation & Consulting Institute, China Electricity Council, Beijing, China, [3]State Key Laboratory of Resources and Environmental Information System, Institute of Geographic Sciences and Natural Resources Research, Chinese Academy of Sciences, Beijing, China, [4]School of Geographical Sciences, Nanjing University of Information Science & Technology, Nanjing, China, [5]Department of Atmospheric Science, School of Environmental Studies, China University of Geosciences, Wuhan, China, [6]Laboratory for Climate Studies, National Climate Center, China Meteorological Administration, Beijing, China, [7]Institute of Urban Meteorology, China Meteorological Administration, Beijing, China

Abstract Taking the megacity of Beijing as an example, a short-time Fourier transform (STFT) method was employed to extract the multi-timescale evolution pattern of the canopy urban heat island intensity (CUHII) during 2000–2020. The STFT of CUHII showed a close relationship between the evolution of the CUHII in Beijing and the background meteorological forcing at intra-annual, weather and intra-daily scales. The intra-annual-scale spectrum of CUHII exhibited an increasing trend with obvious seasonal variation of the canopy urban heat island (CUHI). The intra-daily-scale spectrum of CUHII showed an increasing trend with the nighttime CUHI developing faster. Increasing Western Pacific Subtropical High intensity can enhance the seasonal and diurnal fluctuations of CUHII. The weather-scale spectrum of CUHII is controlled by weather system evolution, showing that the frequency of cold/heat waves (CWs/HWs) in Beijing was significantly negatively correlated with the weather-scale spectral intensity of the CUHII. CWs and HWs can increase the CUHII for a long duration.

Plain Language Summary The canopy urban heat island (CUHI) phenomenon can affect human health and the ecological environment, and its multi-timescale variability brings great uncertainty to the study of urban climates worldwide. In this study, taking the megacity of Beijing as an example, a novel short-time Fourier transform (STFT) method was used to extract the multi-timescale pattern of the CUHI intensity (CUHII) during 2000–2020. The STFT of CUHII showed a close relationship between the CUHI and the background meteorological forcing at intra-annual, weather and intra-daily scales. The intra-annual spectrum of CUHII showed an increasing trend with a V-shaped mode. The local climatic backgrounds of different cities can lead to differences in the seasonal development of the CUHI. The intra-daily spectrum of CUHII showed an increasing trend due to the asymmetry in the day/night development of the CUHI. Increasing Western Pacific Subtropical High Intensity can enhance the seasonal and diurnal fluctuations of CUHII. The weather-scale spectrum of CUHII was mainly controlled by weather system evolution, showing that cold waves and heat waves can increase the CUHII over a long duration. Our findings indicate that the evolution of CUHII is a nonlinear and complex process that is directly related to multi-timescale background climate forcing.

1. Introduction

Urbanization changes the surface energy balance and hydrological balance in urban areas, such as increasing the absorption of solar radiation and reducing evaporation (Luo & Lau, 2021; Sun et al., 2016; Xue et al., 2023), resulting in higher temperatures in urban areas than in surrounding rural areas. This phenomenon is called the urban heat island (UHI) effect. This study focuses on the UHI of the urban canopy layer—namely, the canopy layer UHI (canopy urban heat island (CUHI)). The CUHI can affect human health and the ecological environment, including various negative effects such as increased mortality risk and energy consumption (Cui et al., 2017; Santamouris, 2014), and deterioration of water and air quality (Zheng et al., 2018). There is a rising risk of urban

Writing – original draft: Longrui Zhang, Fu Luo
Writing – review & editing: Longrui Zhang, Fu Luo, Guitao Pan, Wenjie Zhang, Guoyu Ren, Yuanjian Yang

heat extremes under both global change and regional/local urbanization (H. Zhang et al., 2023; Zong, Yang, et al., 2021; Zong et al., 2022), therefore, it has been widely studied and discussed globally.

Current research on the causes of CUHI formation mainly focuses on the analysis of anthropogenic factors, including anthropogenic heat discharge (Kato & Yamaguchi, 2005; Shahmohamadi et al., 2011), urban underlying surface changes (Zhou & Chen, 2018; C. Zhao et al., 2018), building structure (Erdem Okumus & Terzi, 2021; Yuan et al., 2020), and atmospheric aerosols (Cao et al., 2016; Han et al., 2020; Y. Yang et al., 2020). However, changes in background weather and climate fields can also directly affect the CUHI (Y. Yang et al., 2022, 2023), resulting in temporal fluctuations of the CUHI phenomenon (Varentsova & Varentsov, 2021). The intensity of the CUHI phenomenon varies depending on the season, month, and weather conditions (Chow & Roth, 2006; Haashemi et al., 2016; Kidder & Essenwanger, 1995). Extreme weather conditions can lead to an extreme CUHI (D. Li & Bou-Zeid, 2013; J. Yang & Bou-Zeid, 2018), which can pose serious threats to the safety of urban residents (Y. Li et al., 2020). However, research on the multi-timescale fluctuations of the CUHI is still relatively scarce, and the effects of weather conditions on the CUHI at different time scales remain unclear. Currently, few studies on the evolution of the CUHI have considered changes in background meteorological fields, but they usually use annually or monthly averaged temperature fields as the research object, which cannot cover changes in weather conditions at other time scales (Deilami et al., 2018; Du et al., 2016; Y. Li et al., 2020). Therefore, an effective method is urgently needed to extract and analyze the evolutionary patterns of the multi-timescale fluctuations of CUHI intensity (CUHII), particularly the synoptic-scale CUHI fluctuations that are most closely related to background atmospheric activities.

The traditional Fourier transform is an effective method for studying periodic oscillations. It can expand any frequency spectrum in the frequency domain to obtain spectral intensity characteristics. The CUHII has seasonal/diurnal fluctuations or weekly fluctuations caused by weather changes and human activities, which can be displayed on a Fourier spectrum. However, the classical Fourier transform can only be expanded in the frequency domain and can only provide the average intensity of fluctuations over the total time period, without revealing the evolution of CUHI fluctuations over time. The short-time Fourier transform (STFT) is a development of the traditional Fourier transform, which enables it to expand in the time domain to obtain the changing features of a given spectral intensity over time (Dobson & Wilson, 1992; Grasser et al., 2010; Mirabal et al., 2002). Therefore, the STFT can reveal fluctuations at different scales, such as seasonal and diurnal fluctuations over time. In addition to these scales, this study further analyzes the changes in the weather-scale frequency of the CUHII, which is closely related to the background meteorological forcing. Therefore, analyzing the variation of CUHII at this weather scale allows for further exploration of the influence of large-scale climate variability on local CUHI.

Accordingly, this study takes the megacity of Beijing as an example, and employs the STFT method to analyze the temporal variations in the CUHII at different time scales (2000–2020), to reveal its relationship with climate variability. In addition, considering that extreme weather situations are more likely to lead to the occurrence of an extreme CUHI, this study further analyzes the correlation between cold waves (CWs) or HWs and the STFT spectrum intensity to reveal the mechanism driving extreme CUHI fluctuations at the weather scale.

2. Data and Methods

Beijing, the capital of China, is an inland city with a high population density, and is surrounded by mountains on three sides in the west, north and northeast, while the southeast is a plain sloping toward the Bohai Sea (Figure 1a). In this study, 2-m ground layer (i.e., canopy layer) temperature data with a 3-hr time interval were selected from seven meteorological stations in the Beijing area covering the period 2000–2020 (http://data.cma.cn/en). The classification of urban and rural stations followed the method of Wang et al. (2013), and their locations are shown in Figure 1a. In this study, the average temperature of all urban stations was used to represent the urban temperature (T_{u}), and the average temperature of all rural stations was used to represent the rural temperature (T_{r}). The CUHII is defined as

$$\mathrm{CUHII} = \Delta T = T_{\mathrm{u}} - T_{\mathrm{r}}.$$

The CUHII was studied for each season: spring (March-May), summer (June-August), autumn (September-November), and winter (December-February). The selected meteorological stations included four urban stations [Haidian (54399), Fengtai (54514), Shijingshan (54513), and Nansanhuan (54511)] and three rural stations [Pinggu (54424), Miyun (54416), and Huairou (54419)].

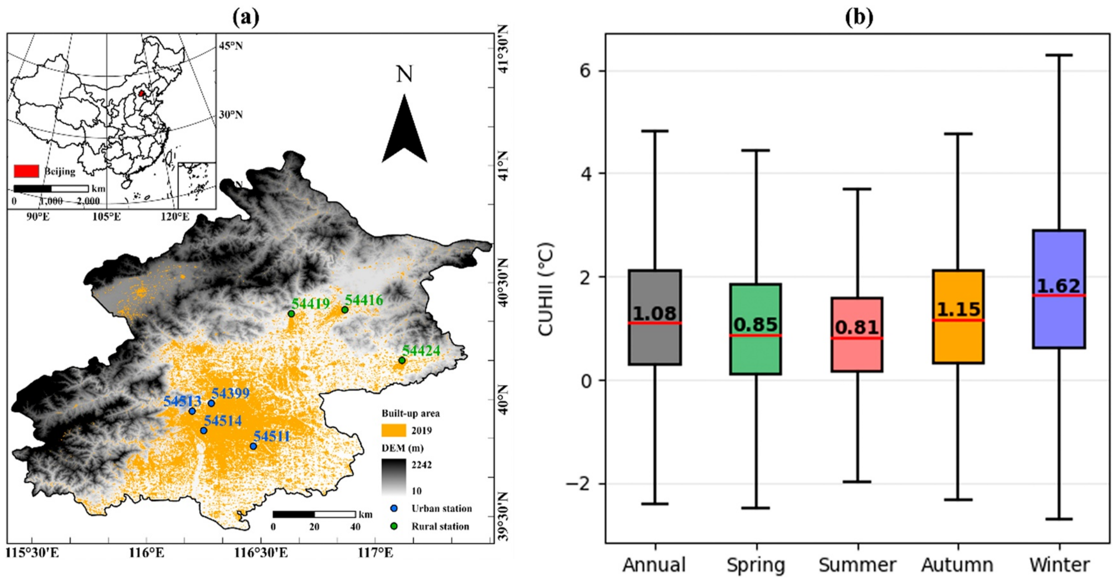

Figure 1. (a) Map of Beijing city and the distribution of urban and rural stations. The selected meteorological stations included four urban stations [Haidian (54399), Fengtai (54514), Shijingshan (54513), and Nansanhuan (54511)] and three rural stations [Pinggu (54424), Miyun (54416), and Huairou (54419)]. (b) Boxplot of Beijing's canopy urban heat island intensity from 2000 to 2020. The line in the middle of the box plot represents the median of the data, the upper and lower edges of the box represent the upper quartile and lower quartile of the data, and the upper and lower whiskers represent the maximum and minimum values of the data.

Rapid urbanization has induced a significant CUHI effect in Beijing in recent years (Figure 1b), with a significantly higher CUHII in winter than in other seasons. Furthermore, its extreme values are also greater in winter than in other seasons, with the CUHII being lowest in summer and its extreme values also the smallest.

The Fourier transform can be used to obtain the fluctuation characteristics of the studied variable at any time scale during the total time period. The formula is as follows:

$$P(v) = \frac{1}{L_t} \int_{t_b}^{t_e} T(t) \cdot e^{-i2\pi vt} \mathrm{d}t, \tag{1}$$

where $T(t)$ is a time series function with a 3-hr time interval between 2000 and 2020; $t \in [t_b, t_e]$, in which t_b is the start time and t_e is the end time; L_t is the length of the time series $T(t)$; v is the frequency, which is the reciprocal of the corresponding fluctuation period; and $P(v)$ is the Fourier spectrum value, which is a complex number. Its complex form is represented as

$$P(v) = \frac{1}{L_t}(P_1(v) + iP_2(v)). \tag{2}$$

The magnitude of the spectrum amplitude is

$$|P(v)| = \frac{1}{L_t}\sqrt{P_1{}^2(v) + P_2{}^2(v)}. \tag{3}$$

In previous studies, the periodogram was often used to analyze the Fourier spectrum instead of P(v) (Bloomfield & Nychka, 1992; Fredriksen & Rypdal, 2016). The periodogram is defined as

$$S(v) = \frac{1}{L_t}\left(P_1{}^2(v) + P_2{}^2(v)\right) = |P(v)|^2 \cdot L_t. \tag{4}$$

This is because, compared with the spectrum amplitude $P(v)$, the periodogram $S(v)$ can provide higher contrast data of the Fourier spectrum.

However, the Fourier spectrum can only reflect information in the frequency domain and cannot obtain the frequency changes with time. Therefore, the STFT method was developed. The STFT is based on the Fourier transform and is used to obtain the Fourier spectrum intensity of a specific frequency in a time period $[t_j, t_j + L_{tw}]$ by continuously shifting the time period. When using the STFT, directly truncating the signal (adding a rectangular window) will cause frequency leakage, so it is necessary to add a non-rectangular window (i.e., multiplying the original function by a window function) to improve the frequency leakage situation. The window function $h(t)$ chosen in this study is the Hamming window:

$$h(t) = 0.54 - 0.46\cos\left(\frac{2\pi(t - t_b)}{L_{tw} - 1}\right). \tag{5}$$

Here t_b is the initial time point of the selected window.

Therefore, at a given frequency v, the STFT is represented as

$$P_v(t_j) = \frac{1}{L_{tw}} \int_{t_j - \frac{1}{2}L_{tw}}^{t_j + \frac{1}{2}L_{tw}} T(t) \cdot h(t) \cdot e^{-i2\pi v\left(t - t_j + \frac{1}{2}L_{tw}\right)} \mathrm{d}t, j = 1, \ldots, N. \tag{6}$$

In this study, the STFT was applied to temperature data for Beijing from 2000 to 2020. $T(t)$ is the time series function with a 3-hr interval between 2000 and 2020. Taking $L_{tw} = 5$ yr, the first window is [2000, 2005] and the last window is [2016, 2020]. Therefore, the time period analyzed by the STFT is from 2002 to 2018.

To obtain the contribution of weather-scale (2–14 days) processes to temperature changes, the spectral intensity of the weather scale is defined as follows:

$$W_v(t_j) = \sum_{0.067 \le v \le 0.5} |S_v(t_j)| = L_{tw} \sum_{0.067 \le v \le 0.5} |P_v(t_j)|^2, j = 1, \ldots, N. \tag{7}$$

3. Results

3.1. Time Series of the CUHI at Various Time Scales

From Figure 2, it can be seen that the temperature time series of urban and rural areas in Beijing exhibit regular intra-annual (i.e., seasonal) periodic changes, and the amplitude is relatively regular (Figures 2a and 2b). The CUHII also shows seasonal periodic changes, but its amplitude fluctuation is larger than that of temperature (Figure 2c). Figure 2d shows that the CUHII in Beijing exhibits seasonal fluctuations and a significant increasing inter-annual trend (0.408°C/10a, $p < 0.01$), and this trend also has seasonal differences (Figures 2e–2h). The CUHII in spring, summer, autumn, and winter shows a significant increasing trend in each case, with trends of 0.468°C/10a, 0.227°C/10a, 0.448°C/10a, and 0.615°C/10a, respectively. Among them, the linear growth trend in winter is the fastest, while that in summer is the slowest. This seasonal discrepancy in growth is further discussed in Section 3.2.

3.2. Fourier and STFT Spectrum for the CUHI

The Fourier transform was applied to the CUHII in Beijing for the period 2000–2020 and the resultant spectrum is shown in Figure 3a. As can be seen, there are significant peaks at $\nu = 1/365\ \mathrm{d}^{-1}$ and $\nu = 1\ \mathrm{d}^{-1}$ (i.e., the intra-annual and intra-daily scales, respectively). Similarly, there are some small peaks between $\nu = 1/2\ \mathrm{d}^{-1}$ and $\nu = 1/14\ \mathrm{d}^{-1}$, representing the periodicity of 2–14 days, which is known as the weather scale in meteorology. The other peaks represent specific periodic oscillations, such as the seasonal scale, which is not covered in this paper but could be studied in future research.

The STFT was applied to the CUHII time series data from 2000 to 2020 using Equation 6, as shown in Figure 3b. The intra-daily-scale ($\nu = 1\ \mathrm{d}^{-1}$) short-time Fourier spectrum was analyzed (Figure 3b) and showed a gradually increasing trend ($p < 0.01$), indicating asymmetry in the temperature changes between day and night and a greater difference in CUHII between daytime and nighttime. The physical explanation for this is that the increasing amount of heat-retaining materials in cities, such as tall buildings and concrete, leads to more sensible heat exchange and heating of the lower atmosphere owing to longwave radiation and temperature differences at night, resulting in a slower decrease in urban canopy nighttime temperature and an increase in nighttime heat island intensity (Kłysik & Fortuniak, 1999; Maahn et al., 2014). In addition to this, previous research has shown that

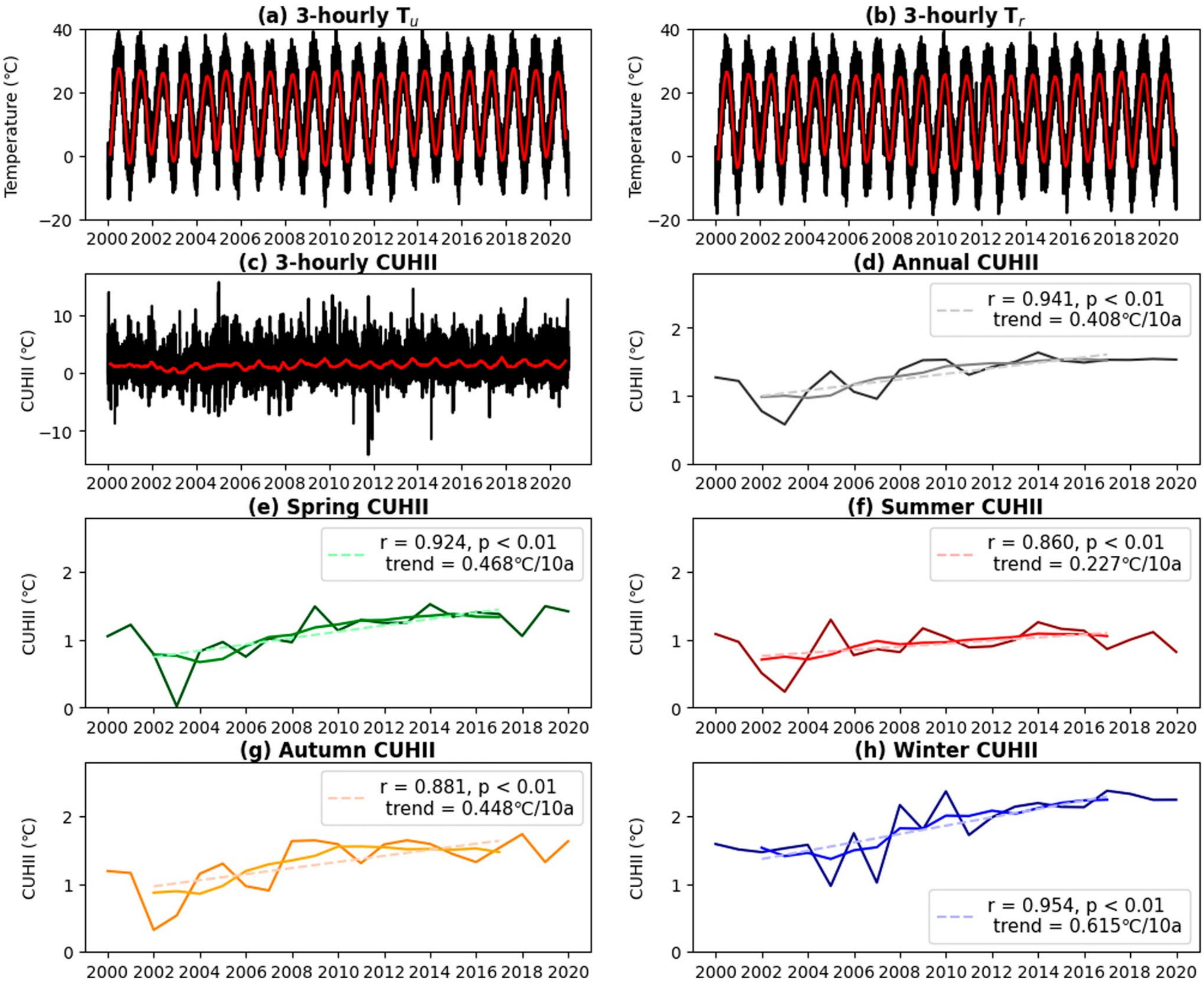

Figure 2. Time series plots of temperature and canopy urban heat island intensity (CUHII) in Beijing from 2000 to 2020. Panels (a)–(c) show the 3-hourly time series of urban temperature (T_u), rural temperature (T_r), and CUHII, respectively, with the black line indicating the original data and the red line indicating the 90-day moving average of the data. Panels (d)–(h) show the annual average urban heat island intensity for the entire year and for each season, with the dark solid line indicating the original annual average data, the light solid line indicating the 5-year moving average of the data, and the lighter dashed line indicating the linear regression line of the light solid line.

urbanization-induced haze weather also strengthens the nighttime heat island intensity (Cao et al., 2016; Y. Yang et al., 2020), which is consistent with the STFT spectrum obtained for diurnal cycles.

The intra-annual-scale ($\nu = 1/356\ \mathrm{d}^{-1}$) STFT spectrum (Figure 3b) shows that the spectral intensity does not vary linearly but exhibits a V-shaped pattern, with a turning point in 2005 ($t1$ in Figure 3b). Before 2005, the spectral intensity shows a decreasing trend, while after 2005 it shows an increasing trend. The V-shaped pattern in Figure 3b can be explained by the seasonal asymmetry in heat island intensity changes described in Section 3.1. Before 2005, the winter heat island intensity decreases slightly, and then after 2005 increases significantly (from 1.370 to 2.264°C, a growth rate of 65.3%), while the summer heat island intensity only shows a slight increase (from 0.750 to 0.987°C, a growth rate of 31.6%). This seasonal asymmetry in CUHII changes results in an increase in the difference between the winter and summer CUHII, which leads to the V-shaped spectrum. This asymmetrical growth is related to the effect of background meteorological forcing. Based on this, it is possible to identify a longer-scale climatic phenomena that can impact temperature variability in the Beijing CUHII.

Western Pacific Subtropical High (WPSH) is a typical climatic phenomenon that influences East Asian climate and environment patterns (Zong, Yang, et al., 2021), in this study, we conducted a correlation analysis

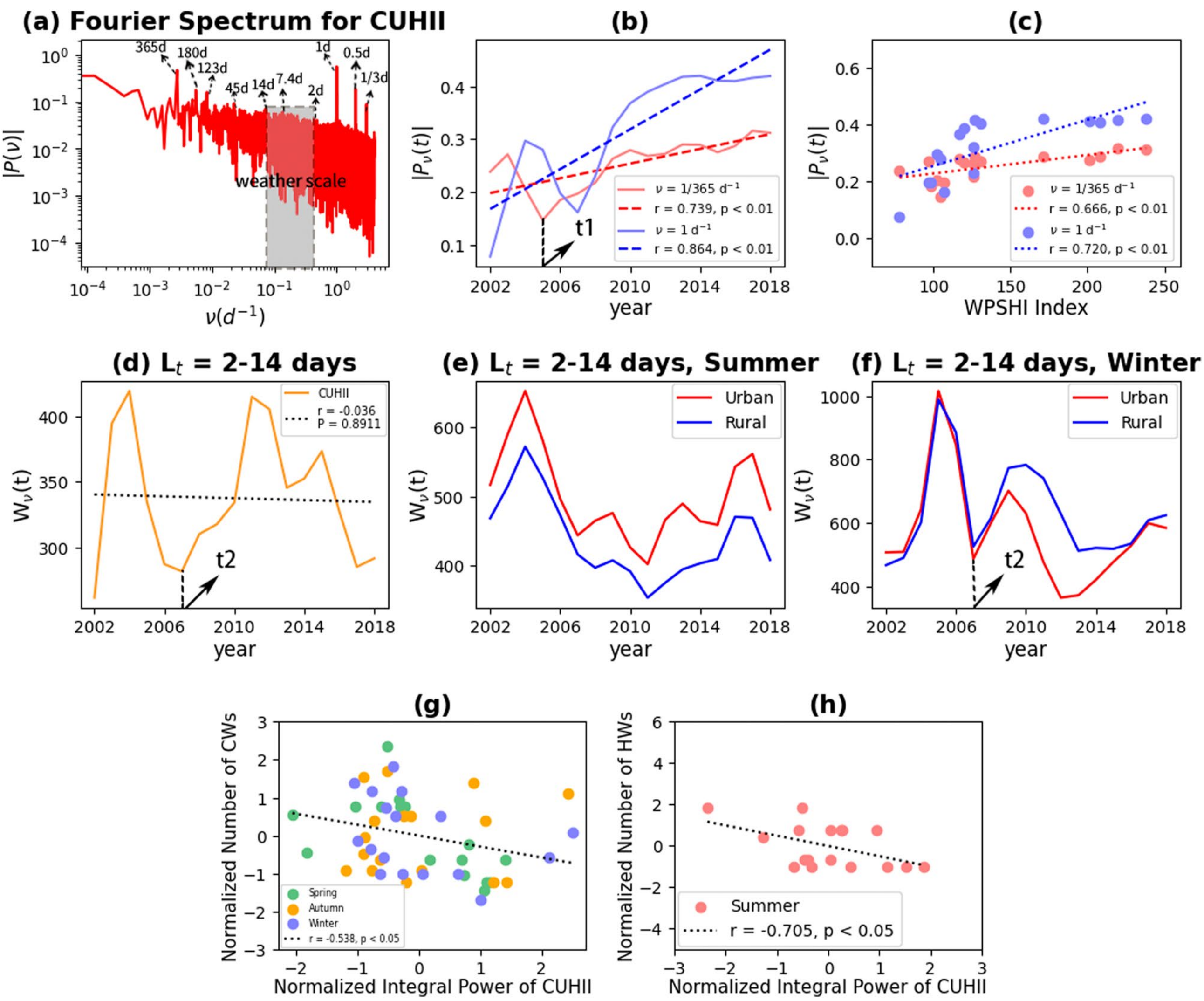

Figure 3. (a) Fourier transform spectrum of the canopy urban heat island intensity (CUHII) from 2000 to 2020, with numbers on the arrows indicating the corresponding peak frequencies. The gray box highlights parts of the important time scales. (b) The short-time Fourier transform (STFT) spectrum of the intra-annual and intra-daily scales, with dashed lines representing the linear fitting. (c) Red dots indicate the relationship between the WPSHI index and the $\nu = 1/365\ \mathrm{d}^{-1}$ STFT spectral intensity, blue dots indicate the relationship between the WPSHI index and the $\nu = 1\ \mathrm{d}^{-1}$ STFT spectral intensity, with dashed lines representing the linear fitting. (d) The STFT of the CUHII in Beijing at the weather scale, with the dashed line representing the linear fit of the data. The weather-scale STFT spectrum of the urban and rural temperature in (e) summer and (f) winter. (g) Scatter plot of the spectral intensity of the weather scale and the number of cold waves in spring (green), autumn (orange), and winter (blue) (all normalized). The dashed line represents the linear fit of all points. (h) Scatter plot of the spectral intensity of the summer weather scale and the number of heat waves (both normalized), in which the dashed line represents the linear fit of all points.

between the yearly-averaged WPSH Intensity (WPSH) index and the STFT spectral intensities of the CUHII at intra-annual-scale and intra-daily-scale. The results reveal a significant positive correlation between the WPSHI index and the spectral intensities at $\nu = 1/356\ \mathrm{d}^{-1}$ and $\nu = 1\ \mathrm{d}^{-1}$ ($r = 0.666/0.720,\ p < 0.01$). Since spectral intensity represents the strength of fluctuations, this finding suggests that the strengthening of WPSH is associated with the enhancement of both seasonal and diurnal variations of the CUHII, which will be discussed in Section 4.

3.3. The Weather-Scale STFT Spectrum

Figure 3d shows the STFT spectrum of the CUHII at the weather scale in Beijing from 2002 to 2018, with a variation period of 2–14 days, which is a scale closely related to the background atmospheric circulation. This study notes that the STFT spectrum of the weather-scale CUHII does not show a significant increasing trend, unlike the intra-annual or intra-daily spectrum. In 2007, it shows a V-shaped pattern similar to the intra-annual spectrum, which can be explained by the STFT spectrum of the temperature (Figures 3e and 3f). In summer, the spectral intensity of T_u is always greater than that of T_r, indicating that cities are more sensitive to temperature fluctuations caused by background weather system changes at the weather scale (Figure 3e). For winter, from 2002 to 2007, the sensitivity of T_u and T_r to background weather system changes at the weather scale is similar. However, from 2007 to 2015, the spectral intensity of T_r is greater (Figure 3f), indicating that T_r fluctuations in response to background meteorological changes are relatively stronger than those of cities, which is opposite to the situation in summer. This leads to the V-shaped pattern in Figure 3b in 2007.

A CW is a typical background meteorological field change on the weather scale. In this study, the criteria of a CW employed by the China Meteorological Administration were selected (namely, a temperature drop of more than 8°C within 24 hr, with a minimum temperature drop to below 4°C; or a temperature drop of more than 10°C within 48 hr, with a minimum temperature drop to below 4°C; or a continuous temperature drop of more than 12°C within 72 hr, with a minimum temperature below 4°C). On this basis, cold-wave data for spring, autumn, and winter in Beijing for the period 2000–2020 were collected and analyzed using a 5-year sliding average. The linear correlation between the cold-wave frequency and the weather-scale STFT spectral intensity of the CUHII was calculated (both were processed as standardized data). As shown in Figure 3g, there was a negative correlation between the cold-wave frequency and the weather-scale STFT spectral intensity ($r = -0.538$, $p < 0.05$), with a stronger negative correlation in the spring ($r = -0.612$, $p < 0.01$). The weather-scale STFT spectral intensity reflects the fluctuations of CUHII on weather-scale time periods. A stronger spectral intensity indicates more prominent variations between the valley and peak values of CUHII, and vice versa. Therefore, the results in Figure 3g suggest that during a CW in Beijing, weather-scale fluctuations of CUHII become less pronounced, resulting in less prominent variations between the troughs and peaks of CUHII at the weather-scale. From a physical perspective, during CW events, the atmosphere is characterized by cold and dry conditions, stable atmospheric stratification, and clear skies, leading to minimal weather changes. This leads to an extended period of elevated CUHII levels (Konstantinov et al., 2018; Varentsova & Varentsov, 2021; J. Yang & Bou-Zeid, 2018), causing the weather-scale fluctuations of CUHII to become less pronounced, thereby weakening the weather-scale spectral intensity of CUHII.

Similarly, the relationship between HWs and the STFT spectrum of summer weather was analyzed. Figure 3h shows a significant negative correlation ($r = -0.705$, $p < 0.05$) between the intensity of the STFT spectrum of the weather scale and the frequency of HWs (5-year moving average). The results suggest that during a HW in Beijing, weather-scale fluctuations of CUHII become less pronounced, resulting in less prominent variations between the valley and peak values of CUHII at the weather scale. From a physical perspective, the high building density in Beijing's urban area, coupled with weak wind speeds, contributes to heat accumulation during HW events. This stored heat is subsequently released as sensible heat during cooling periods, mitigating the cooling impact of weather changes. As a consequence, CUHII remains elevated and sustained at a heightened level for an extended duration (D. Li & Bou-Zeid, 2013; Zong, Liu, et al., 2021). This phenomenon leads to diminished weather-scale fluctuations of CUHII and a reduction in the weather-scale STFT spectral intensity of CUHII.

To test the robustness of this finding, we analyzed the differences in CUHII during the occurrence of CWs/HWs and the 7 days before and after these events (Tables S1 and S2 in Supporting Information S1). We found that the peak (valley) value of CUHII during CW/HW periods is lower (higher) than that in the periods before and after the CWs/HWs, causing the weather-scale fluctuations of CUHII less pronounced.

4. Discussion

From a physical perspective, concerning seasonal fluctuations, Liu et al. (2012) indicated that a strong WPSH often leads to a northward shift in the WPSH's position, and when the location is northerly, the climatological average position of China's rain belts will be raised to the north of the Yellow River, causing summer precipitation will change to more in the north and less in the south. So a strong WPSH increases summer rainfall and humidity in the Beijing area. Huang and Lu (2018) indicated that for the specific region of Beijing, a humid environment is conducive to the attenuation of heat island intensity. Therefore, a strong WPSH effectively reduces the valley values of seasonal fluctuations, making them more prominent. Regarding diurnal fluctuations, due to the dense urbanization in the Beijing area, it stores more heat during HW periods. Moreover, the strengthening of WPSHI also leads to increased stable airflows and aerosol pollution (Dong et al., 2023; Gong & He, 2002; Qu et al., 2013; Wu et al., 2019; Zong et al., 2023). These factors cause the urban area of Beijing to experience weaker nighttime cooling compared to rural areas, resulting in higher peak values for diurnal fluctuations, thereby making diurnal fluctuations more prominent. To test the robustness of our results, the filtering methods of Seasonal-Trend decomposition using LOESS (STL) (Cleveland et al., 1990) and Butterworth Bandpass Filter (BBF) are also selected to extract the seasonal and diurnal fluctuations of CUHII and the annual trend of WPSHI (Figures S1 and S2 in Supporting Information S1).

The seasonal range of the STL-filtered CUHII between winter and summer (winter CUHII minus summer CUHII) and the STL-filtered summer WPSHI exhibits a significant positive correlation ($r = 0.668, p < 0.01$) (Figure S2a in Supporting Information S1) and is highly consistent with the observed relationship between the intra-annual-scale CUHII spectral intensities based on STFT method and WPSHI ($r = 0.666, p < 0.01$) (Figure S2c in Supporting Information S1). These findings suggest that a strong WPSH could make the seasonal fluctuations of CUHII more prominent, which is because the strong WPSH could weaken the summer CUHII in Beijing, leading to a reduction in the valley value of CUHII, while the impact of WPSH on winter CUHII is not obvious. Moreover, the diurnal range of the BBF-filtered summer CUHII (nighttime CUHII minus daytime CUHII) and the STL-filtered summer WPSHI also exhibit significant positive correlation ($r = 0.586, p < 0.01$) (Figure S2b in Supporting Information S1) and is highly consistent with the observed relationship between the intra-daily-scale CUHII spectral intensities based on STFT method and WPSHI ($r = 0.720, p < 0.01$) (Figure S2d in Supporting Information S1). Our findings suggest that a strong WPSH could make the diurnal fluctuations of CUHII more prominent, which is because the strong WPSH could strengthen the nighttime CUHII in Beijing, leading to an increase in the peak value of CUHII, while the impact of WPSH on daytime CUHII is not obvious. The conclusions obtained through STL filtering and BBF filtering are highly consistent with those obtained through the STFT method, thereby further validating the robustness and reliability of the conclusions drawn in this study.

The intra-annual STFT spectrum of the CUHII in Beijing showed a V-shaped pattern owing to the seasonal asymmetry of CUHI development. The winter CUHI developed significantly faster than the summer CUHII (Figures 2e and 2g), over the same period (2000–2020), the WPSHI also displayed an increasing trend (Figure S1 in Supporting Information S1). Considering the negative impact of WPSHI on summer CUHII, it can be inferred that WPSHI contributes to this asymmetrical growth. However, the seasonal asymmetry of CUHI development in Beijing is in contrast to the conclusion of a CUHII study in Moscow (Varentsova & Varentsov, 2021), where the summer weather conditions were found to have become more favorable for CUHII development, with the summer heat island developing faster than the winter CUHI. This suggests that different cities, due to their different local geographic and climatic environments, have different weather conditions that affect the CUHII, which may be due to differences in factors influencing the heat island, such as temperature, humidity, and wind speed, which vary among the same seasons (Priyadarsini et al., 2008; L. Zhao et al., 2014). For Moscow, according to existing research (Gorchakov et al., 2014), the heat island phenomenon will stimulate anticyclonic weather conditions in the Moscow region in reverse, and such conditions are often accompanied by clear and less cloudy weather, which is conducive to the development of the heat island. Therefore, it is a strengthening of the anticyclonic weather conditions in summer that has led to the enhancement of the summer heat island effect in Moscow. For Beijing, existing research shows that it has a higher frequency of temperature inversion in winter (Xu et al., 2020), which can cause pollutants and heat to stay near the ground and not diffuse upward, resulting in an enhancement of the winter heat island effect. These factors have led to the seasonal differences in heat island intensity between the two cities and can be further quantitatively analyzed in future studies.

In addition, the weather-scale spectrum has a potential in directly determining the trend of weather-scale situations, such as cold-air outbreaks, which is different from counting the number of cold-air outbreaks using the standard air temperature drop during a CW. Since the STFT method used in this paper is based on the Fourier principle, it is mathematically continuous, and thus the spectral analysis method can detect any marginal changes in CUHII, and accurately and effectively obtain the relationship between the CUHI and cold-air activities or other trends of change in weather situations. Therefore, for research on other related background forcing of urban climate changes, the STFT method can still be widely adopted.

5. Conclusion

This study used a new STFT method to study the evolution of the CUHI in Beijing at different time scales for the period 2000–2020. Our findings indicate that the evolution of CUHII is a nonlinear and complex process that is directly related to multi-timescale background climate forcing, as follows.

The V-shaped pattern of the intra-annual-scale STFT spectrum of CUHII was analyzed and found to be due to the seasonal asymmetry of CUHI development (31.6% increase in summer after 2005, 65.3% increase in winter), while the continuously increasing trend ($R^2 = 0.75$, $p < 0.05$) of the intra-daily-scale STFT spectrum was attributed to the asymmetry in the development of the day/night CUHII. The weather-scale STFT spectrum, mainly regulated by the weather system's evolution, also exhibited a V-shaped pattern, which was related to the relative sensitivity of T_u and T_r to the evolution of weather systems (rural areas became more sensitive than urban areas in winter after 2007). When analyzing the intra-annual-scale, intra-daily-scale and weather-scale spectrum, it was observed that WPSHI and the frequencies of CWs and HWs significantly influenced the temporal variations of CUHII. WPSHI exhibited positive correlations with intra-annual-scale and intra-daily-scale spectral intensities ($r = 0.666/0.720$, $p < 0.01$), indicating that the diurnal and seasonal fluctuations of CUHII would intensify during periods of strong WPSH. The frequencies of CWs and HWs were negatively correlated to weather-scale spectral intensity ($r = -0.289/-0.497$, $p < 0.05$), and the CUHI phenomenon tended to maintain a high intensity for a long time under these extreme cold and hot weather conditions.

In general, our findings indicate that different local climates in cities can lead to differences in the seasonal development of CUHII, which is directly related to background climate forcing. The use of spectral analysis methods to study meteorological activities (e.g., cold air) and urban boundary layer climate factors (e.g., CUHI), at multiple scales, is highly effective and should therefore be paid more attention in related future research.

Conflict of Interest

The authors declare no conflicts of interest relevant to this study.

Data Availability Statement

The datasets that are analyzed and used to support the findings of this study are available in the public domains: The hourly meteorological data, WPSH data and built-up area date are available at linkage: https://doi.org/10.5281/zenodo.10057770 (L. Zhang, 2023).

Acknowledgments
This research was supported by the National Natural Science Foundation of China (42222503 and 42201053) and supported by a grant from State Key Laboratory of Resources and Environmental Information System. We thank Profs Miao Junfeng and Ning Guicai for valuable comments.

References

Bloomfield, P., & Nychka, D. (1992). Climate spectra and detecting climate change. *Climatic Change*, *21*(3), 275–287. https://doi.org/10.1007/BF00139727

Cao, C., Lee, X., Liu, S., Schultz, N., Xiao, W., Zhang, M., & Zhao, L. (2016). Urban heat islands in China enhanced by haze pollution. *Nature Communications*, *7*(1), 12509. https://doi.org/10.1038/ncomms12509

Chow, W. T. L., & Roth, M. (2006). Temporal dynamics of the urban heat island of Singapore. *International Journal of Climatology*, *26*(15), 2243–2260. https://doi.org/10.1002/joc.1364

Cleveland, R. B., Cleveland, W. S., McRae, J. E., & Terpenning, I. (1990). STL: A seasonal-trend decomposition. *Journal of Official Statistics*, *6*(1), 3–73. Retrieved from https://www.nniiem.ru/file/news/2016/stl-statistical-model.pdf

Cui, Y., Yan, D., Hong, T., & Ma, J. (2017). Temporal and spatial characteristics of the urban heat island in Beijing and the impact on building design and energy performance. *Energy*, *130*, 286–297. https://doi.org/10.1016/j.energy.2017.04.053

Deilami, K., Kamruzzaman, M., & Liu, Y. (2018). Urban heat island effect: A systematic review of spatio-temporal factors, data, methods, and mitigation measures. *International Journal of Applied Earth Observation and Geoinformation*, *67*, 30–42. https://doi.org/10.1016/j.jag.2017.12.009

Dobson, J., & Wilson, M. (1992). Sensitization of oral bacteria in biofilms to killing by light from a low-power laser. *Archives of Oral Biology*, *37*(11), 883–887. https://doi.org/10.1016/0003-9969(92)90058-G

Dong, P., Chen, L., & Yan, Y. (2023). Influence of extratropical cyclones on air quality in Beijing. *Atmospheric Research*, *283*, 106552. https://doi.org/10.1016/j.atmosres.2022.106552

Du, H., Wang, D., Wang, Y., Zhao, X., Qin, F., Jiang, H., & Cai, Y. (2016). Influences of land cover types, meteorological conditions, anthropogenic heat and urban area on surface urban heat island in the Yangtze River Delta Urban Agglomeration. *Science of the Total Environment*, *571*, 461–470. https://doi.org/10.1016/j.scitotenv.2016.07.012

Erdem Okumus, D., & Terzi, F. (2021). Evaluating the role of urban fabric on surface urban heat island: The case of Istanbul. *Sustainable Cities and Society*, *73*, 103128. https://doi.org/10.1016/j.scs.2021.103128

Fredriksen, H.-B., & Rypdal, K. (2016). Spectral characteristics of instrumental and climate model surface temperatures. *Journal of Climate*, *29*(4), 1253–1268. https://doi.org/10.1175/JCLI-D-15-0457.1

Gong, D., & He, X.-Z. (2002). Interdecadal change in western Pacific subtropical high and climatic effects. *Acta Geographica Sinica*, *57*, 185–193. https://doi.org/10.1007/BF02837475

Gorchakov, G., Kadygrov, E., Kunitsyn, V., Zakharov, V., Semutnikova, E., Karpov, A., et al. (2014). The Moscow heat island in the blocking anticyclone during summer 2010. *Doklady Earth Sciences*, *456*(2), 736–740. https://doi.org/10.1134/S1028334X14060233

Grasser, T., Reisinger, H., Wagner, P.-J., Schanovsky, F., Goes, W., & Kaczer, B. (2010). The time dependent defect spectroscopy (TDDS) for the characterization of the bias temperature instability. In *2010 IEEE international reliability physics symposium* (pp. 16–25). https://doi.org/10.1109/IRPS.2010.5488859

Haashemi, S., Weng, Q., Darvishi, A., & Alavipanah, S. K. (2016). Seasonal variations of the surface urban heat island in a semi-Arid city. *Remote Sensing*, *8*(4), 352. https://doi.org/10.3390/rs8040352

Han, W., Li, Z., Wu, F., Zhang, Y., Guo, J., Su, T., et al. (2020). The mechanisms and seasonal differences of the impact of aerosols on daytime surface urban heat island effect. *Atmospheric Chemistry and Physics*, *20*(11), 6479–6493. https://doi.org/10.5194/acp-20-6479-2020

Huang, Q., & Lu, Y. (2018). Long-term trend of urban heat island intensity and climatological affecting mechanism in Bejing city. *Scientia Geographica Sinica*, *38*(10), 1715–1723. Retrieved from http://geoscien.neigae.ac.cn/EN/10.13249/j.cnki.sgs.2018.10.016

Kato, S., & Yamaguchi, Y. (2005). Analysis of urban heat-island effect using ASTER and ETM+ Data: Separation of anthropogenic heat discharge and natural heat radiation from sensible heat flux. *Remote Sensing of Environment*, *99*(1), 44–54. https://doi.org/10.1016/j.rse.2005.04.026

Kidder, S. Q., & Essenwanger, O. M. (1995). The effect of clouds and wind on the difference in nocturnal cooling rates between urban and rural areas. *Journal of Applied Meteorology and Climatology*, *34*(11), 2440–2448. https://doi.org/10.1175/1520-0450(1995)034<2440:TEOCAW>2.0.CO;2

Kłysik, K., & Fortuniak, K. (1999). Temporal and spatial characteristics of the urban heat island of Łódź, Poland. *Atmospheric Environment*, *33*(24), 3885–3895. https://doi.org/10.1016/S1352-2310(99)00131-4

Konstantinov, P., Varentsov, M., & Esau, I. (2018). A high density urban temperature network deployed in several cities of Eurasian Arctic. *Environmental Research Letters*, *13*(7), 075007. https://doi.org/10.1088/1748-9326/aacb84

Li, D., & Bou-Zeid, E. (2013). Synergistic interactions between urban heat islands and heat waves: The impact in cities is larger than the sum of its parts. *Journal of Applied Meteorology and Climatology*, *52*(9), 2051–2064. https://doi.org/10.1175/JAMC-D-13-02.1

Li, Y., Schubert, S., Kropp, J. P., & Rybski, D. (2020). On the influence of density and morphology on the Urban Heat Island intensity. *Nature Communications*, *11*(1), 2647. https://doi.org/10.1038/s41467-020-16461-9

Liu, Y. Y., Li, W. J., Ai, W. X., & Qingquan, L. (2012). Reconstruction and application of the monthly western Pacific subtropical high indices. *J. Appl. Meteor. Sci.*, *23*, 414–423. (in Chinese). https://doi.org/10.3969/j.issn.1001-7313.2012.04.004

Luo, M., & Lau, N. C. (2021). Increasing human-perceived heat stress risks exacerbated by urbanization in China: A comparative study based on multiple metrics. *Earth's Future*, *9*(7), e2020EF001848. https://doi.org/10.1029/2020ef001848

Maahn, M., Burgard, C., Crewell, S., Gorodetskaya, I. V., Kneifel, S., Lhermitte, S., et al. (2014). How does the spaceborne radar blind zone affect derived surface snowfall statistics in polar regions? *Journal of Geophysical Research: Atmospheres*, *119*(24), 13604–13620. https://doi.org/10.1002/2014JD022079

Mirabal, Y. N., Chang, S. K., Atkinson, E. N., Malpica, A. M., Follen, M., & Richards-Kortum, R. R. (2002). Reflectance spectroscopy for in vivo detection of cervical precancer. *Journal of Biomedical Optics*, *7*(4), 587–594. https://doi.org/10.1117/1.1502675

Priyadarsini, R., Hien, W. N., & Wai David, C. K. (2008). Microclimatic modeling of the urban thermal environment of Singapore to mitigate urban heat island. *Solar Energy*, *82*(8), 727–745. https://doi.org/10.1016/j.solener.2008.02.008

Qu, W., Wang, J., Gao, S., & Wu, T. (2013). Effect of the strengthened western Pacific subtropical high on summer visibility decrease over eastern China. *Journal of Geophysical Research (Atmospheres)*, *118*(13), 7142–7156. https://doi.org/10.1002/jgrd.50535

Santamouris, M. (2014). Cooling the cities—A review of reflective and green roof mitigation technologies to fight heat island and improve comfort in urban environments. *Solar Energy*, *103*, 682–703. https://doi.org/10.1016/j.solener.2012.07.003

Shahmohamadi, P., Che-Ani, A. I., Maulud, K. N. A., Tawil, N. M., & Abdullah, N. A. G. (2011). The impact of anthropogenic heat on formation of urban heat island and energy consumption balance. *Urban Studies Research*, *2011*, 1–9. https://doi.org/10.1155/2011/497524

Sun, Y., Zhang, X., Ren, G., Zwiers, F. W., & Hu, T. (2016). Contribution of urbanization to warming in China. *Nature Climate Change*, *6*(7), 706–709. https://doi.org/10.1038/nclimate2956

Varentsova, S. A., & Varentsov, M. I. (2021). A new approach to study the long-term urban heat island evolution using time-dependent spectroscopy. *Urban Climate*, *40*, 101026. https://doi.org/10.1016/j.uclim.2021.101026

Wang, J., Yan, Z., Li, Z., Liu, W., & Wang, Y. (2013). The impact of urbanization on extreme temperatures in Beijing in the past 30 years. *Scientific Bulletin*, *58*(33), 3464–3470. https://doi.org/10.1360/csb2013-58-33-3464

Wu, X., Xu, L., Hong, Y., Chen, J., Qiu, Y., Hu, B., et al. (2019). The air pollution governed by subtropical high in a coastal city in Southeast China: Formation processes and influencing mechanisms. *Science of the Total Environment*, *692*, 1135–1145. https://doi.org/10.1016/j.scitotenv.2019.07.341

Xu, W., Wen, Z., Shang, B., Dore, A. J., Tang, A., Xia, X., et al. (2020). Precipitation chemistry and atmospheric nitrogen deposition at a rural site in Beijing, China. *Atmospheric Environment*, *223*, 117253. https://doi.org/10.1016/j.atmosenv.2019.117253

Xue, J., Zong, L., Yang, Y., Bi, X., Zhang, Y., & Zhao, M. (2023). Diurnal and interannual variations of canopy urban heat island (CUHI) effects over a mountain–valley city with a semi-arid climate. *Urban Climate*, *48*, 101425. https://doi.org/10.1016/j.uclim.2023.101425

Yang, J., & Bou-Zeid, E. (2018). Should cities embrace their heat islands as shields from extreme cold? *Journal of Applied Meteorology and Climatology*, *57*(6), 1309–1320. https://doi.org/10.1175/JAMC-D-17-0265.1

Yang, Y., Guo, M., Wang, L., Zong, L., Liu, D., Zhang, W., et al. (2023). Unevenly spatiotemporal distribution of urban excess warming in coastal Shanghai megacity, China: Roles of geophysical environment, ventilation and sea breezes. *Building and Environment*, *235*, 110180. https://doi.org/10.1016/j.buildenv.2023.110180

Yang, Y., Min, G., Ren, G., Liu, S., Zong, L., Zhang, Y., et al. (2022). Modulation of wintertime canopy urban heat island (CUHI) intensity in Beijing by synoptic weather pattern in planetary boundary layer. *Journal of Geophysical Research: Atmospheres*, *127*(8), e2021JD035988. https://doi.org/10.1029/2021JD035988

Yang, Y., Zheng, Z., Yim, S. Y. L., Roth, M., Ren, G., Gao, Z., et al. (2020). PM2.5 pollution modulates wintertime urban heat island intensity in the Beijing-Tianjin-Hebei Megalopolis, China. *Geophysical Research Letters*, *47*(1), e2019GL084288. https://doi.org/10.1029/2019GL084288

Yuan, C., Adelia, A. S., Mei, S., He, W., Li, X.-X., & Norford, L. (2020). Mitigating intensity of urban heat island by better understanding on urban morphology and anthropogenic heat dispersion. *Building and Environment*, *176*, 106876. https://doi.org/10.1016/j.buildenv.2020.106876

Zhang, H., Luo, M., Pei, T., Liu, X., Wang, L., Zhang, W., et al. (2023). Unequal urban heat burdens impede climate justice and equity goals. *Innovation*, *4*(5), 100488. https://doi.org/10.1016/j.xinn.2023.100488

Zhang, L. (2023). Ground-based observation in Beijing and WPSH data from the article "Elucidating the multi-timescale variability of a canopy urban heat island by using the short-time Fourier transform" [Dataset]. Zenodo. https://doi.org/10.5281/zenodo.10057770

Zhao, C., Jensen, J., Weng, Q., & Weaver, R. (2018). A geographically weighted regression analysis of the underlying factors related to the surface urban heat island phenomenon. *Remote Sensing*, *10*(9), 1428. https://doi.org/10.3390/rs10091428

Zhao, L., Lee, X., Smith, R. B., & Oleson, K. (2014). Strong contributions of local background climate to urban heat islands. *Nature*, *511*(7508), 216–219. https://doi.org/10.1038/nature13462

Zheng, Z., Ren, G., Wang, H., Dou, J., Gao, Z., Duan, C., et al. (2018). Relationship between fine-particle pollution and the urban heat island in Beijing, China: Observational evidence. *Boundary-Layer Meteorology*, *169*(1), 93–113. https://doi.org/10.1007/s10546-018-0362-6

Zhou, X., & Chen, H. (2018). Impact of urbanization-related land use land cover changes and urban morphology changes on the urban heat island phenomenon. *Science of the Total Environment*, *635*, 1467–1476. https://doi.org/10.1016/j.scitotenv.2018.04.091

Zong, L., Liu, S., Yang, Y., Ren, G., Yu, M., Zhang, Y., & Li, Y. (2021). Synergistic influence of local climate zones and wind speeds on the urban heat island and heat waves in the megacity of Beijing, China. *Frontiers in Earth Science*, *9*, 673786. https://doi.org/10.3389/feart.2021.673786

Zong, L., Yang, Y., Gao, M., Wang, H., Wang, P., Zhang, H., et al. (2021). Large-scale synoptic drivers of co-occurring summertime ozone and $PM_{2.5}$ pollution in eastern China. *Atmospheric Chemistry and Physics*, *21*(11), 9105–9124. https://doi.org/10.5194/acp-21-9105-2021

Zong, L., Yang, Y., Xia, H., Gao, M., Sun, Z., Zheng, Z., et al. (2022). Joint occurrence of heatwaves and ozone pollution and increased health risks in Beijing, China: Role of synoptic weather pattern and urbanization. *Atmospheric Chemistry and Physics*, *22*(10), 6523–6538. https://doi.org/10.5194/acp-22-6523-2022

Zong, L., Yang, Y., Xia, H., Yuan, J., & Guo, M. (2023). Elucidating the impacts of various atmospheric ventilation conditions on local and trans-boundary ozone pollution patterns: A case study of Beijing, China. *Journal of Geophysical Research: Atmospheres*, *128*(20), e2023JD039141. https://doi.org/10.1029/2023jd039141